Available online at www.sciencedirect.com

SCIENCE DIRECT®

International Journal of Heat and Mass Transfer 49 (2006) 1310–1319

International Journal of HEAT and MASS TRANSFER

www.elsevier.com/locate/ijhmt

An optimized reciprocity Monte Carlo method for the calculation of radiative transfer in media of various optical thicknesses

Francis Dupoirieux [a,*], Lionel Tessé [a], Sébastien Avila [a], Jean Taine [b]

[a] Fundamental and Applied Energetics Department (DEFA), Office National d'Études et de Recherches Aérospatiales, Chemin de la Hunière, 91761 Palaiseau Cedex, France

[b] Laboratoire d'Énergétique Moléculaire et Macroscopique, Combustion (EM2C), École Centrale Paris, 92295 Châtenay-Malabry Cedex, France

Received 27 July 2005; received in revised form 7 October 2005
Available online 6 December 2005

Abstract

An efficient Monte Carlo method for the calculation of radiative transfer in complex geometry systems including semi-transparent media has been achieved and validated. This method, which is based on the reciprocity principle and called optimized reciprocity method (ORM), can be applied to systems discretized in a large number of cells. For each pair of elementary cells exchanging radiative energy, the transfer calculation is carried out by minimizing, for a given computational time, the standard deviation of the radiative power or of the wall flux. The results obtained with ORM have been successfully compared to those obtained with previous approaches in a numerical benchmark.

1. Introduction

The idea to use the Monte Carlo method to calculate radiative transfer in participating media is old [1–6] but the use of this method becomes common [7] due to the increase of computer power.

In many papers [8–11], the Monte Carlo method is only used as a reference to validate other conventional discretization methods. Nowadays it is used directly to solve problems including complex physics, such as turbulence-radiation interaction [12–14], scattering [15], polarized radiative transfer [16,17] or complex geometry, sometimes in conjunction with deterministic methods [18,19].

Many techniques of variance reduction have been developed in order to reduce the computation time [20–23]. One of these techniques consists in using the radiation reciprocity principle, either from the geometrical point of view only [24–27] or from both geometrical and energetical points of view [28–34]. Paper [30] deals with two reciprocal approaches which have specific application fields. The emission reciprocity method (ERM) is designed to limit the calculation to the only part of the domain where the solution is sought. This method is also well adapted to calculate the radiative power or flux in zones where the temperature is high. On the other hand, the absorption reciprocity method (ARM) is well adapted for low temperature zones but requires a calculation over the complete domain. These methods are in particular more efficient than the conventional forward Monte Carlo Method (FM) in case of large optical thickness or weak temperature gradient. However, in current cases of moderate optical thickness and high temperature gradients (radiating combustion gases, for instance) none of the three methods give the lowest standard deviation in the whole calculation domain. In particular, the suitable method to calculate wall fluxes is in general different from the one adapted to calculate radiative powers [30].

The aim of the present work is to develop and validate an optimized hybrid approach able to give good results, for wall fluxes and radiative powers, in media of various optical thicknesses. This optimized reciprocity method (ORM) is obtained by selecting, for each power exchange between two cells (elementary volumes or surfaces), the

* Corresponding author.
E-mail address: francis.dupoirieux@onera.fr (F. Dupoirieux).

0017-9310/$ - see front matter © 2005 Elsevier Ltd. All rights reserved.
doi:10.1016/j.ijheatmasstransfer.2005.10.009

Nomenclature

$A_{\nu qj}$	fraction of power emitted from cell q that is absorbed in cell j (non-dimensional)
i	cell index
j	index of a cell exchanging power with the reference cell q
I_ν^0	equilibrium (or blackbody) spectral intensity (Wm^{-2} (cm^{-1})$^{-1}$ sr^{-1})
K	proportionality constant ((W/cm^{-1})$^{-1}$)
L_w	distance between the walls in the test cases (m)
N	total number of optical paths
N_{calc}	number of independent calculations used to estimate the standard deviation in the test cases
N_S	number of elementary surfaces in the system
N_V	number of elementary volumes in the system
N_x	number of cells in x direction (i.e. between the walls) in the test cases
$N_{\nu q}$	number of optical paths originating from cell q at wavenumber ν
$P_q(i)$	probability that a fraction of the power emitted from cell q is absorbed in cell i
P_q	total radiative power in cell q (W)
P_{qj}^{exch}	total power exchanged between cells q and j (W)
$P_{\nu qj}^{exch}$	spectral power exchanged between cells q and j (W/cm^{-1})
$P_{\nu qj}^{ERM}$	spectral power exchanged between cells q and j involved in the calculation of P_q with the emission reciprocity method (W/cm^{-1})
$P_{\nu qj}^{ARM}$	spectral power exchanged between cells q and j involved in the calculation of P_q with the absorption reciprocity method (W/cm^{-1})
q	index of the reference cell
S_q	elementary surface q
T_c	temperature at the center of the medium in the test cases (K)
T_w	wall temperature in the test cases (K)
V_q	elementary volume q
x	spatial coordinate along the direction orthogonal to the walls
$X(i)$	crenel function applied to cell i

Greek symbols

$\alpha_{\nu jc}$	spectral absorptivity for the cth crossing of cell j (non-dimensional)
ε_g	equivalent total emissivity of the medium in the test cases (non-dimensional)
ε_w	gray emissivity of the walls in the test cases (non-dimensional)
$\varepsilon_{\nu i}$	spectral emissivity of surface i (non-dimensional)
$\kappa_{\nu q}$	spectral absorption coefficient in cell q (m^{-1})
ν	wavenumber (cm^{-1})
$\sigma(Q)$	standard deviation of quantity Q
τ_ν	spectral transmissivity (non-dimensional)

Subscript

w	refers to a wall

Notation

$\widetilde{(\ )}$	Monte Carlo statistical estimation (average over the contributions of the optical paths)

reciprocal method giving the lowest standard deviation for this exchange.

ORM is detailed in Section 2. Results of benchmark calculations obtained from ERM, ARM, FM and ORM are compared and discussed in Section 3.

2. Optimized reciprocity method (ORM)

A general reciprocity Monte Carlo method requires the stochastic calculation of all quantities P_{ij}^{exch}, the total radiative powers exchanged between any couple (i,j) of elementary cells in the system. These cells are volume or surface elements resulting from a geometrical discretization. At present, this general approach is not suitable for systems of complex geometries discretized in a large number of cells for two reasons: (i) for a standard 3D calculation, the required computing storage, proportional to the number of cells squared, would be too large; (ii) the number of optical paths joining two cells would be generally too small to obtain an accurate enough value of the exchanged power. Consequently, we do not consider here this general approach, but methods such as the emission reciprocity method (ERM) and the absorption reciprocity method (ARM) [30], in which the radiative power in a given cell q is obtained directly without accurate calculation and storage of all P_{qj}^{exch}, where j is the index of each cell exchanging with q. Before detailing the optimized reciprocity method (ORM), a brief outline of ERM and ARM is given hereafter.

The total radiative power P_q in a cell q is obtained by summing up powers P_{qj}^{exch} exchanged between this cell and all surrounding cells j:

$$P_q = \sum_{j=1}^{N_V+N_S} P_{qj}^{exch} = -\sum_{j=1}^{N_V+N_S} P_{jq}^{exch}. \tag{1}$$

In this equation, N_S and N_V stand for the number of elementary surfaces and volumes, respectively. Hereafter, only exchanges between elementary volumes V_q and V_j are detailed; exchanges between elementary surfaces or between elementary surface and volume are treated in Appendix A.

The total exchanged power P^{exch}_{qj} is given by

$$P^{\text{exch}}_{qj} = \int_0^{+\infty} P^{\text{exch}}_{vqj}\, \mathrm{d}v, \tag{2}$$

where v is the wavenumber and P^{exch}_{vqj} the spectral exchanged power given by

$$P^{\text{exch}}_{vqj} = 4\pi V_q \kappa_{vq}\left(I^0_{vj} - I^0_{vq}\right)A_{vqj}. \tag{3}$$

Quantity κ_{vq} is the spectral absorption coefficient in cell q and I^0_{vq} the equilibrium spectral intensity in the cell q. P^{exch}_{vqj} is strictly equal to zero when I^0_{vj} and I^0_{vq} are equal. According to Eq. (5) of Ref. [30], A_{vqj} is defined by

$$A_{vqj} = \frac{1}{4\pi V_q}\int_{V_q}\int_{4\pi}\sum_{c=1}^{N_p}\tau_v(BF_c)\alpha_{vjc}\,\mathrm{d}\Omega_q\,\mathrm{d}V_q. \tag{4}$$

Index c ($c = 1,\ldots,N_p$) relates to the serial number of crossings of cell j by a given optical path issued from cell q, taking into account reflections on the walls. Quantity τ_v (BF_c) is the spectral global transmission factor, taking into account possible wall reflections, between the source point B in cell q and F_c, the cth inlet point in cell j of a given optical path, as shown in Fig. 1 of Ref. [30]. Quantity α_{vjc} is the spectral absorptivity corresponding to the cth crossing of cell j. In these circumstances, A_{vqj} is the fraction of the spectral power emitted from cell q, i.e. $4\pi V_q\kappa_{vq}I^0_{vq}$, that is absorbed in cell j. It is the only quantity that must be stochastically calculated in the expression of P^{exch}_{vqj}.

In Monte Carlo methods, the stochastically generated optical paths are associated with the emission of radiative energy from the origin cell and the absorption of a part of this energy in an arrival cell. ERM derives from the first equality in Eq. (1). Forward optical paths issued from the considered cell q and reverse optical paths issued from all crossed cells j are considered, as shown in Fig. 3 of Ref. [30], to give the stochastic estimation $\widetilde{A}_{vqj}$ of A_{vqj}. Hereafter, all stochastic estimations of the physical quantities are noted with a tilde. Therefore, the spectral power exchanged between cells q and j and involved in the calculation of P_q with ERM writes

$$\widetilde{P}^{\text{ERM}}_{vqj} = 4\pi V_q\kappa_{vq}\left(I^0_{vj} - I^0_{vq}\right)\widetilde{A}_{vqj}. \tag{5}$$

On the other hand, in ARM which derives from the second equality in Eq. (1), forward optical paths issued from all cells j and crossing the considered cell q and reverse optical paths issued from cell q are used as shown in Fig. 4 of Ref. [30]. Consequently, the spectral power exchanged between cells q and j and involved in the calculation of P_q with ARM writes

$$\widetilde{P}^{\text{ARM}}_{vqj} = 4\pi V_j\kappa_{vj}\left(I^0_{vj} - I^0_{vq}\right)\widetilde{A}_{vjq}. \tag{6}$$

It is worth noticing that, in the limit case of large numbers, the following equation expressing the reciprocity principle can be derived from Eqs. (5) and (6):

$$\kappa_{vq}V_qA_{vqj} = \kappa_{vj}V_jA_{vjq}. \tag{7}$$

The optimization of the radiative power calculation in a given cell q can be obtained by an optimization of the calculation of each power exchange between the cell q and any current cell j of the domain. In ORM, each power exchange is calculated with the best approach between ARM and ERM, i.e. the approach that leads to the lowest standard deviation of its stochastic estimation. Because of the (i) and (ii) given in the beginning of this Section, all these standard deviations cannot be calculated accurately and stored but their mathematical expressions can be compared. From Eqs. (5), (6), it results that the standard deviations of the two methods are given by

$$\sigma\left(\widetilde{P}^{\text{ERM}}_{vqj}\right) = 4\pi V_q\kappa_{vq}\left|I^0_{vj} - I^0_{vq}\right|\sigma\left(\widetilde{A}_{vqj}\right), \tag{8}$$

$$\sigma\left(\widetilde{P}^{\text{ARM}}_{vqj}\right) = 4\pi V_j\kappa_{vj}\left|I^0_{vj} - I^0_{vq}\right|\sigma\left(\widetilde{A}_{vjq}\right). \tag{9}$$

In these equations, $\sigma(Q)$ stands for the standard deviation of quantity Q.

In terms of probability, A_{vqj} can be written as the following mathematical expectation:

$$A_{vqj} = \sum_{i=1}^{N_V+N_S} X(i)P_q(i), \tag{10}$$

where $N_V + N_S$ is the total number of cells, P_q (i) is the probability that a fraction of the power emitted from cell q is absorbed in cell i and X is a function of index i defined as follows: $X(i) = 1$ if $i = j$, $X(i) = 0$ if $i \neq j$. In other words, A_{vqj} is equal to $P_q(j)$. The standard deviation of the function X of which A_{vqj} is the mathematical expectation is given by

$$\sigma_0 = \sqrt{\sum_{i=1}^{N_V+N_S}\left[X(i) - A_{vqj}\right]^2 P_q(i)}. \tag{11}$$

Using the definition of function X, the fact that $P_q(j)$ is equal to A_{vqj} and that the sum $\sum_i P_q(i)$ is equal to 1, it comes

$$\sigma_0 = \sqrt{A_{vqj}\left(1 - A_{vqj}\right)}. \tag{12}$$

By assuming that A_{vqj} is small compared to 1, which is true in particular if cell j is optically thin, the previous standard deviation writes

$$\sigma_0 = \sqrt{A_{vqj}}. \tag{13}$$

The stochastic estimation $\widetilde{A}_{vqj}$ of A_{vqj} is obtained by averaging the numerical results over a large number of optical paths which are generated from q, independently, with the same probability law. According to the central limit theorem, the standard deviation of this stochastic estimation is given by

$$\sigma\left(\widetilde{A}_{vqj}\right) = \frac{\sigma_0}{\sqrt{N_{vq}}} = \sqrt{\frac{A_{vqj}}{N_{vq}}}, \tag{14}$$

where N_{vq} is the number of optical paths originating from cell q at wavenumber v. If the most common method, called non-uniform distribution method (NUD) is used (see [30]), the number $N_{\nu q}$ is proportional to the spectral power emitted from cell q. When q is a volume, $N_{\nu q}$ is then equal to $4\pi\kappa_{\nu q}V_q I^0_{\nu q}K$, where K is a proportionality constant independent of index q. From this relation and from Eqs. (14) and (8), it comes

$$\sigma\left(\widetilde{P}^{\mathrm{ERM}}_{\nu qj}\right) = \frac{\sqrt{4\pi V_q \kappa_{\nu q} A_{\nu qj}}\left|I^0_{\nu j} - I^0_{\nu q}\right|}{\sqrt{K I^0_{\nu q}}}. \tag{15}$$

In the same way, Eq. (9) yields

$$\sigma\left(\widetilde{P}^{\mathrm{ARM}}_{\nu qj}\right) = \frac{\sqrt{4\pi V_j \kappa_{\nu j} A_{\nu jq}}\left|I^0_{\nu j} - I^0_{\nu q}\right|}{\sqrt{K I^0_{\nu j}}}. \tag{16}$$

Taking into account Eq. (7), the ratio of these standard deviations writes

$$\frac{\sigma\left(\widetilde{P}^{\mathrm{ERM}}_{\nu qj}\right)}{\sigma\left(\widetilde{P}^{\mathrm{ARM}}_{\nu qj}\right)} = \sqrt{\frac{I^0_{\nu j}}{I^0_{\nu q}}}. \tag{17}$$

From this equation, it results that the lowest standard deviation is obtained with ERM when temperature T_q in cell q is larger than temperature T_j in cell j and with ARM in the opposite case. Therefore, the spectral exchanged power $P^{\mathrm{exch}}_{\nu qj}$, involved in the calculation of P_q, is calculated with ERM when T_q is larger than T_j and from the ARM in the opposite case. Note that the criterion for the ERM-ARM selection is not rigorous when one of the cells is not optically thin but in this case the numerical tests will assess the method.

3. Results and discussion

The ORM is validated by comparison with the ERM, ARM and FM in the same benchmark as in Ref. [30]. Two parallel infinite opaque walls separated by a non-isothermal emitting and absorbing medium are considered. The local radiative power depends only on the spatial coordinate x along the direction orthogonal to the walls and is given, as well as fluxes on the walls, by well-known analytical expressions (see [35], Eq. (VII.110) or [36]) which will be taken as reference solutions. Of course, even if the fields are 1D, the optical paths are calculated in the 3D physical space and the infinite character of the transverse dimensions is simulated by total specular reflection conditions on the boundaries parallel to the x axis.

Eight cases corresponding to different temperature profiles and different wall or medium absorption conditions have been treated. These cases are summarized in Table 1, in which the values of the distance L_w between the walls and of the wall emissivity ε_w are given. In all cases, the temperature profile $T(x)$ has a symmetric parabolic shape but different values of T_c, the temperature of the medium center, and T_w, the wall temperature, have been considered. The distance between the walls is discretized in $N_x = 20$ small intervals. The number N of optical paths has been adjusted for each case in order to obtain the same calculation time of 400 s with a single SGI R12000 processor. This number, which depends on the global optical thickness, is given in Table 1. The computations have been split into $N_{\mathrm{calc}} = 400$ independent calculations of the whole domain in order to determine the standard deviation of the numerical results including local radiative power and wall fluxes. Table 1 gives also the global optical thickness κL_w for each case involving a gray medium and the total emissivity ε_g of the medium obtained with the Hottel charts [37] for the cases involving actual gases, here modeled by a CK approach. For these cases, the first and the second values of ε_g correspond to the total emissivities of the whole medium assumed to be isothermal, respectively at T_c and T_w. Table 2 gives the calculated wall fluxes for all the cases. Values in parentheses are the standard deviations.

All the comparisons regard the standard deviation for a given computation time. Since the standard deviation decreases as the square root of the optical path number, the ratio of the computation times of two different methods for a given calculation accuracy is equal to the square of the ratio of their standard deviations obtained in the above-mentioned conditions. Consequently this ratio strongly depends on the considered spatial cell.

3.1. Case of a gray medium

Although no actual medium is gray, the gray assumption is useful since it allows the optical thickness of a medium to be accurately controlled.

Table 1
Benchmark cases

	Case 1	Case 2	Case 3	Case 4	Case5	Case 6	Case 7	Case 8
κL_w	2	0.1	5	40	2	2	Actual gases	Actual gases
L_w (m)	0.2	0.2	0.2	0.2	0.2	0.2	0.2	4
ε_g	0.86	0.10	0.99	1	0.86	0.86	0.03–0.15	0.19–0.50
ε_w	0.8	0.8	0.8	0.8	0.8	0.8	1	1
T_c (K)	2500	2500	2500	2500	500	300	2500	2500
T_w (K)	500	500	500	500	2500	290	500	500
N_x (N_{calc})	20(400)	20(400)	20(400)	20(400)	20(400)	20(400)	20(400)	20(400)
$N \times 10^{-6}$	1	0.2	1.44	7	1	1	1	1.8
t (s)	≈400	≈400	≈400	≈400	≈400	≈400	≈400	≈400

Table 2
Mean radiative fluxes on the walls (standard deviations in parentheses)

	Reference	FM	ERM	ARM	ORM
Case 1 (kW/m^2)	560.5	554.9 (17.5)	562.0 (123)	554.9 (17.4)	554.9 (17.4)
Case 2 (kW/m^2)	159.9	159.6 (5.53)	159.8 (42.4)	159.7 (5.51)	159.8 (5.51)
Case 3 (kW/m^2)	294.5	294.5 (12.9)	290.6 (133)	294.5 (12.7)	294.5 (12.7)
Case 4 (kW/m^2)	11.20	13.84 (5.40)		11.03 (4.00)	11.03 (4.00)
Case 5 (kW/m^2)	−1306	−1310 (18.4)	−1305 (4.02)	−1293 (245)	−1305 (4.02)
Case 6 (W/m^2)	24.26	21.54 (11.8)	24.22 (0.27)	24.05 (0.87)	24.22 (0.27)
Case 7 (kW/m^2)	54.04	53.99 (2.33)	51.47 (58.7)	53.99 (2.28)	53.99 (2.28)
Case 8 (kW/m^2)	195.9	195.6 (11.9)	234.0 (1842)	195.6 (11.8)	195.7 (11.9)

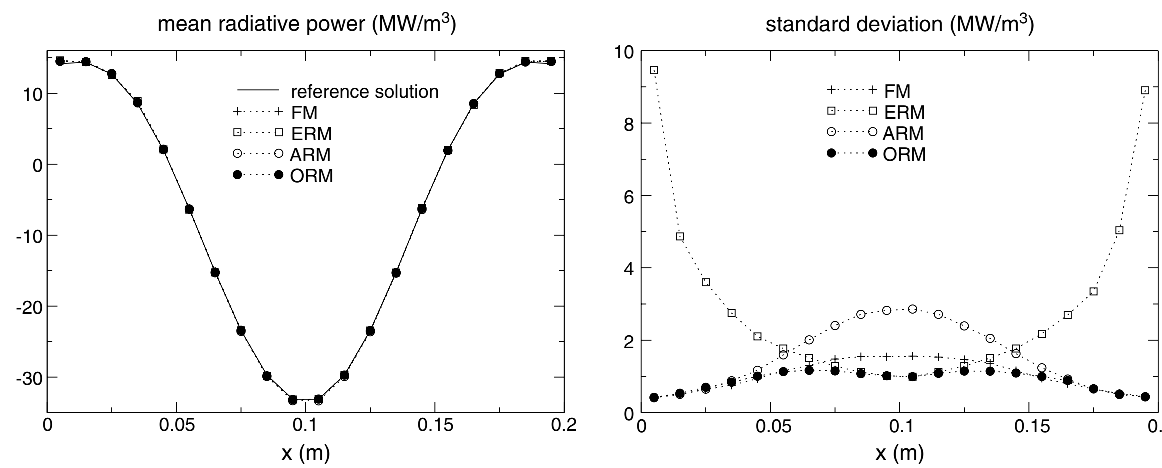

Fig. 1. Mean radiative power profile and standard deviation in case 1.

Cases 1–4 are related to cold walls separated by a hot medium and differ from one another in optical thickness. In case 1, which corresponds to a global optical thickness equal to 2, the radiative power profiles obtained with the four methods are in good agreement with the reference solution as shown in Fig. 1. The lowest standard deviation is obtained with ORM. Concerning the wall fluxes, the standard deviations obtained with ORM, ARM and FM are equal and low. ERM leads to a much larger confidence interval. The similarity of the wall fluxes given by ARM and ORM arises from the fact that, in an energy exchange between a wall elementary surface and an elementary volume of high temperature, the ARM contribution is chosen to calculate the wall flux with ORM. Moreover, the power received by a wall surface is calculated in the same way for FM and ARM. The emitted power is not identically calculated in both methods but, since this emitted power is low, because of the locally low temperature, FM, ARM and consequently ORM give similar results on the walls.

Case 2 corresponds to a low optical thickness of 0.1. Fig. 2 shows that ORM is the best of the reciprocity methods for the radiative power but FM leads to the lowest standard deviation. It has already been shown in Ref. [30] that a medium of low optical thickness with strong temperature gradients is not favorable to global reciprocity methods. However, even in these unfavorable circumstances, ORM can be considered as satisfactory. ERM gives no value for $x = 0.5$ cm and $x = 19.5$ cm. Indeed, the power emitted by the cells close to the walls is small because of both low temperature and optical thickness. Since, in the NUD approach, optical paths are distributed in cells according to the emitted power, no optical path is generated from the cells close to the walls. For the wall flux, the conclusion is the same as in case 1, with good results obtained with ORM, ARM and FM.

Case 3 corresponds to an optical thickness of 5. For both radiative power and wall flux, ORM is the most accurate as shown in Fig. 3 and Table 2. The standard deviation obtained with ARM is now smaller than the one obtained with FM in the center of the medium. As in case 1, near the walls, the standard deviation obtained with ERM becomes very high while FM and ARM have the same behavior as ORM. Concerning the flux on the walls, ARM and ORM give the same value with the same lowest standard deviation, in very good agreement with the reference value. FM gives almost the same value with a slightly higher standard deviation. The value given by ERM is too low and its standard deviation is much higher than with the other methods.

Case 4 deals with a very high optical thickness of 40. The radiative powers and the wall flux calculated by FM are not satisfactory as shown in Fig. 4 and Table 2. Indeed, when the optical thickness is very high, only neighboring cells exchange energy. Therefore, the energy transfer

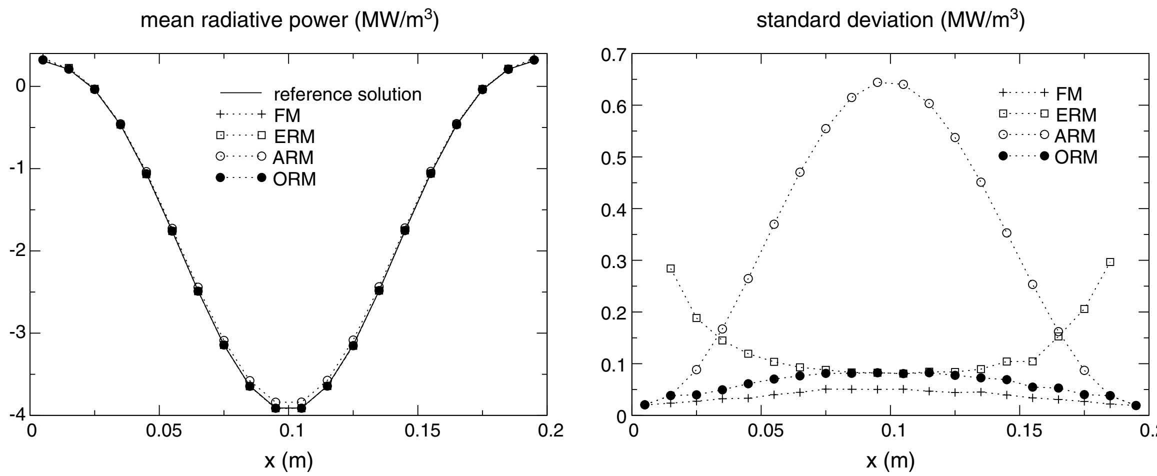

Fig. 2. Mean radiative power profile and standard deviation in case 2.

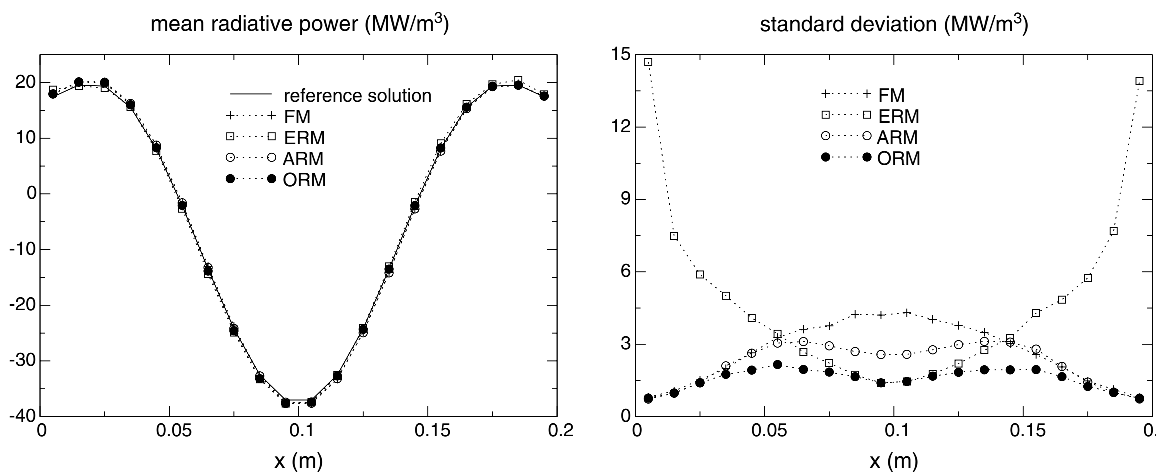

Fig. 3. Mean radiative power profile and standard deviation in case 3.

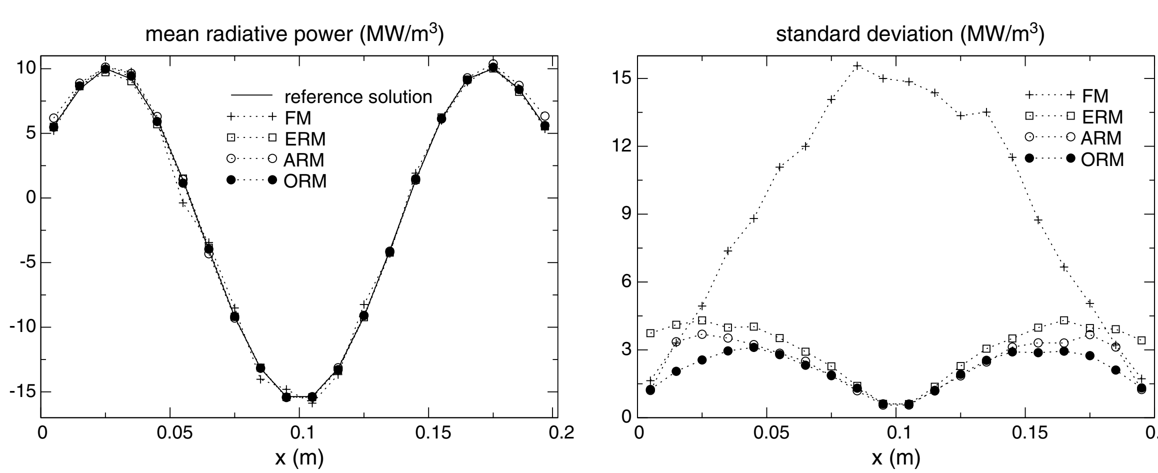

Fig. 4. Mean radiative power profile and standard deviation in case 4.

involves cells of similar temperature and in that case reciprocity methods are much more efficient than FM. The standard deviations for ERM and ARM have the same order of magnitude except near the walls where ARM works better. The lowest standard deviation is everywhere obtained with ORM. Due to the strong absorption in elementary volumes, each optical path is very short and the calculation of the corresponding trajectory requires a small computation time. Therefore, for a same computation time, the number of tracked optical paths is much larger in that case than in the other cases (see Table 1). On the other hand, optical paths that do not leave the origin cell do not contribute to the results. In the NUD approach considered here, all the optical paths are issued from volume elements. Consequently, ERM does not give results related to the wall flux. For the wall flux, as in case 3, ARM and ORM give exactly the same results and work a little better than FM.

Case 5 is similar to case 1 concerning the optical thickness but the temperature profile has been changed to give a cold central medium and hot walls. ORM and FM lead to the best results for the radiative power as shown in Fig. 5. With regard to the wall flux, ORM gives the best results together with ERM, insofar as the exchange between a hot wall element and an elementary volume is calculated here in the same way in ORM and ERM.

In case 6, the temperature gradients are small and the optical thickness is the same as in case 1. This case is favorable to reciprocity methods because the energy is exchanged between cells of similar temperatures as for the optically thick medium of case 4. Consequently, FM leads to poor results as shown in Fig. 6 and Table 2. The radiative powers obtained with ORM are more accurate than those obtained with ERM and similar to those calculated by ARM. For the wall flux, ORM and ERM give the best results.

3.2. Case of a real gas

Case 7 is related to real gases with the same temperature profile and distance between the walls as in case 1. The gas is a CO_2–H_2O–N_2 mixture at atmospheric pressure. The molar fractions of CO_2 and H_2O are respectively 0.116 and 0.155. These conditions are typical of those existing in flames and combustion flows. Gas radiative properties are treated in a correlated manner by a CK model

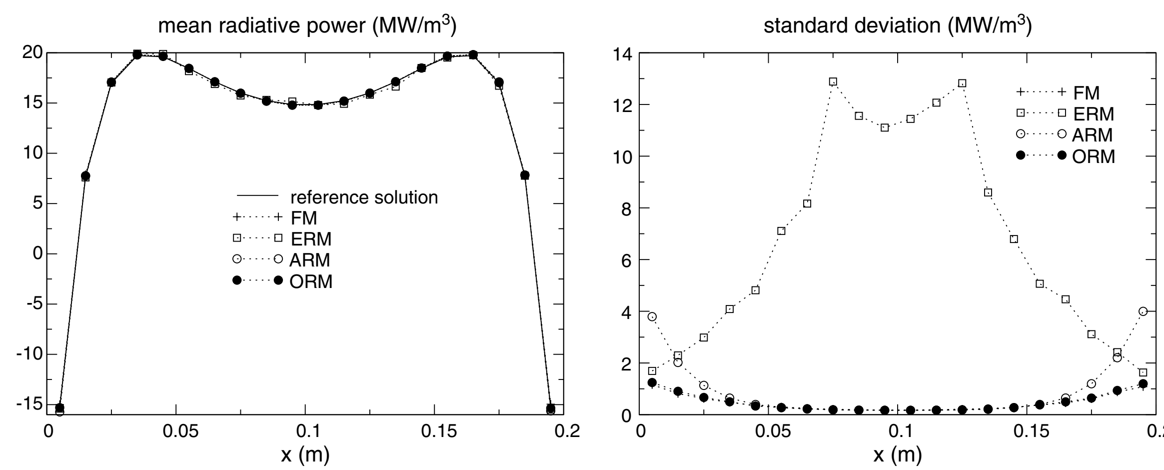

Fig. 5. Mean radiative power profile and standard deviation in case 5.

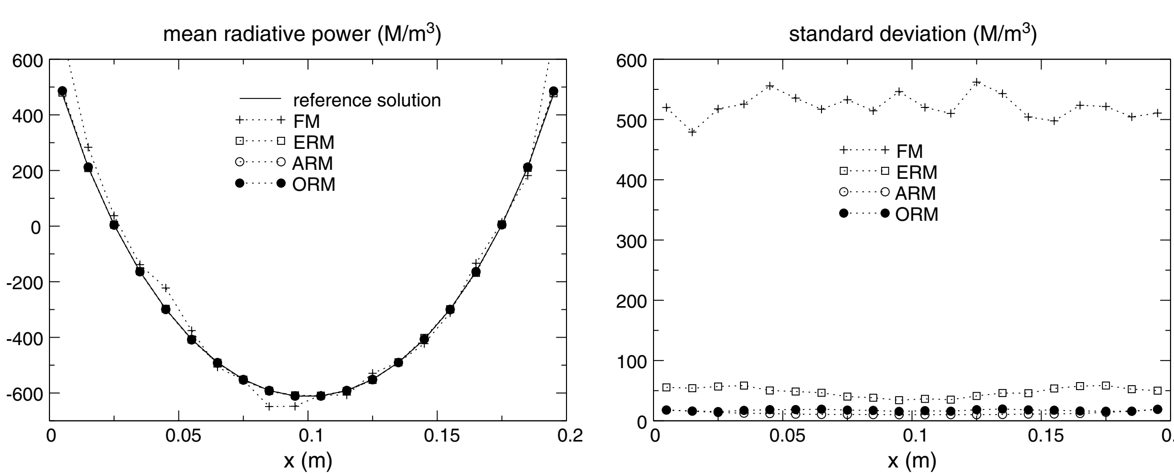

Fig. 6. Mean radiative power profile and standard deviation in case 6.

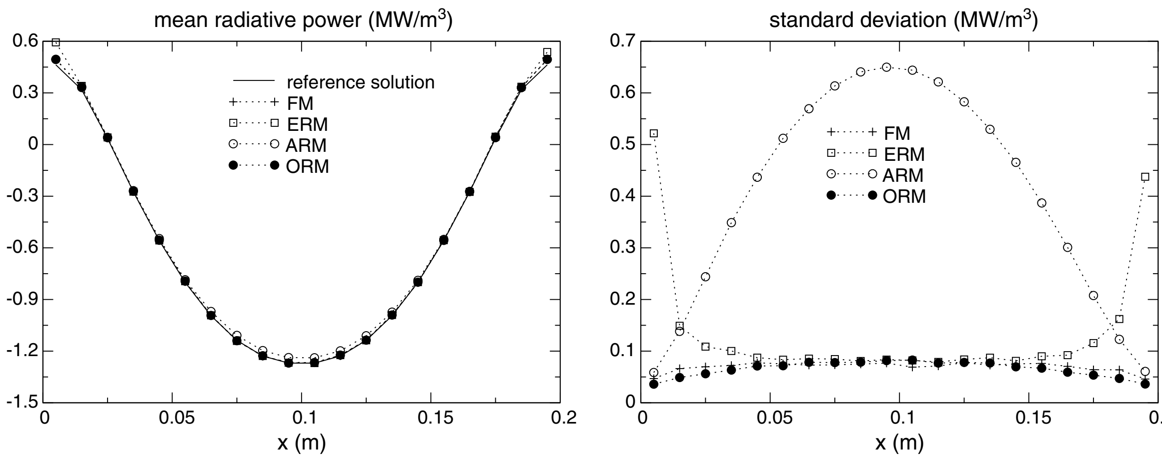

Fig. 7. Mean radiative power profile and standard deviation in case 7.

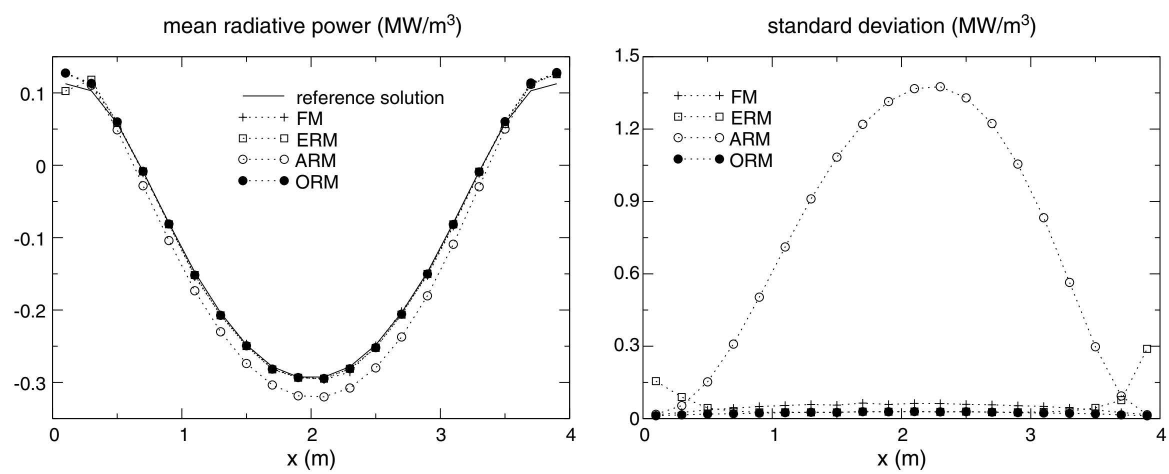

Fig. 8. Mean radiative power profile and standard deviation in case 8.

[38–41] based on the parameters taken in Ref. [42]. According to the values of the total emissivity ε_g, obtained from Hottel charts [37] for the extreme temperatures, and given in Table 1, case 7 corresponds to an optically thin medium as case 2. Concerning the radiative power, ORM and FM lead to the best results as shown in Fig. 7. ARM does not give good results in the center of the medium and ERM does not work well near the walls. As predicted, this behavior is the same as in case 2. For the wall flux, ORM leads also to the best results together with ARM and FM, as shown in Table 2. The fact that ORM, ARM and FM give very similar results on the walls is due to the low temperature of these walls.

Case 8 is also related to real gases and differ from case 7 through the distance between the walls which is now equal to 4 m. From the point of view of the total emissivity of the medium, this case is intermediate between cases 2 and 1, as shown in Table 1. For the calculation of radiative power in this case, the conclusion of our previous paper [30] was to use ARM near the walls and ERM in the center of the medium because there was no method able to give good results everywhere. The conclusion of this work is more satisfactory since ORM gives everywhere the best results for the radiative power, as shown in Fig. 8. Concerning the wall flux, ORM, ARM and FM are the best approaches.

4. Conclusion

The Monte Carlo optimized reciprocity method (ORM) for the calculation of radiative transfer in complex semi-transparent media has been achieved and validated. The method consists, for each exchange between two elementary cells, in the selection of the best method between the emission reciprocity method (ERM) and the absorption reciprocity method (ARM) developed in a previous work. A simple criterion has been analytically obtained to control the ERM–ARM selection. For a given computational time, the standard deviation of the radiative power or of the wall flux obtained by the ORM is smaller than those obtained by other methods (ARM, ERM and forward method) in almost all cases of a numerical benchmark. The ratio of the computation times of two different methods for a given calculation accuracy is equal to the square of the ratio of these standard deviations. Consequently this ratio strongly depends on the considered spatial cell. For a small optical thickness the ORM performs significantly better than the ARM in the center of the medium and much better than the ERM near the walls. The conclusion is the same for a real gas. For a high optical thickness, the ORM has only a slightly better behavior than the ERM and ARM in the center of the medium but performs much better than these methods near the walls. It is worth noting that the ORM leads to accurate results both for radiative power and wall flux unlike the ARM, the ERM and the forward Monte Carlo method.

Appendix A. Treatment of the power exchange in the case of elementary surfaces

In the general case, whatever the type of the elementary cells, volume or surface, Eqs. (5) and (6) can be rewritten as

$$\widetilde{P}_{\nu qj}^{\mathrm{ERM}} = C_q\left(I_{\nu j}^0 - I_{\nu q}^0\right)\widetilde{A}_{\nu qj}, \tag{18}$$

$$\widetilde{P}_{\nu qj}^{\mathrm{ARM}} = C_j\left(I_{\nu j}^0 - I_{\nu q}^0\right)\widetilde{A}_{\nu jq}, \tag{19}$$

where C_i $(i = q,j)$ is equal to $4\pi V_i\kappa_{\nu i}$ when i is an elementary volume and equal to $\pi S_i\varepsilon_{\nu i}$ when i is an elementary surface S_i; $\varepsilon_{\nu i}$ is the spectral emissivity of S_i; $A_{\nu qj}$, the fraction of the power emitted from q and absorbed in j, is given by Eq. (4) when both cells q and j are elementary volumes. When q is an elementary surface and j an elementary volume, $A_{\nu qj}$ becomes, with the same formalism as in Eq. (4)

$$A_{\nu qj} = \frac{1}{\pi S_q}\int_{S_q}\int_{2\pi}\sum_{c=1}^{N_p}\tau_\nu(BF_c)\alpha_{\nu jc}\cos\theta\,\mathrm{d}\Omega_q\,\mathrm{d}S_q, \tag{20}$$

where θ is the angle between the normal unit vector of q and the ray. The summation on $\mathrm{d}\Omega_q$ is made only on the 2π solid angle containing the calculation domain. When q is an elementary volume and j an elementary surface, $A_{\nu qj}$ is defined by

$$A_{\nu qj} = \frac{1}{4\pi V_q}\int_{V_q}\int_{4\pi}\sum_{c=1}^{N_p}\tau_\nu(BF_c)\varepsilon_{\nu j}\,\mathrm{d}\Omega_q\,\mathrm{d}V_q \tag{21}$$

and, when both cells q and j are elementary surfaces, $A_{\nu qj}$ is defined by

$$A_{\nu qj} = \frac{1}{\pi S_q}\int_{S_q}\int_{2\pi}\sum_{c=1}^{N_p}\tau_\nu(BF_c)\varepsilon_{\nu j}\cos\theta\,\mathrm{d}\Omega_q\,\mathrm{d}S_q. \tag{22}$$

Eqs. (18) and (19) imply that, for a large number of optical paths,

$$C_qA_{\nu qj} = C_jA_{\nu jq}. \tag{23}$$

Equations similar to Eqs. (8), (9), (15) and (16) can be obtained by replacing $4\pi V_q\kappa_{\nu q}$ by C_q and $4\pi V_j\kappa_{\nu j}$ by C_j. From these equations, Eq. (17) can be deduced whatever the type of the cells q and j.

References

[1] J.R. Howell, M. Perlmutter, Monte Carlo solution of thermal transfer through radiant media between gray walls, J. Heat Transfer 86 (1964) 116–122.

[2] P.M. Campbell, Monte Carlo method for radiative transfer, Int. J. Heat Mass Transfer 10 (1967) 519–527.

[3] J.R. Howell, Application of Monte Carlo to heat transfer problems, Adv. Heat Transfer 5 (1968) 1–54.

[4] L.L. House, L.W. Avery, The Monte Carlo technique applied to radiative transfer, J. Quant. Spectrosc. Radiat. Transfer 9 (1969) 1579–1591.

[5] A. Haji-Sheikh, E.M. Sparrow, Probability distributions and error estimates for Monte Carlo solutions of radiation problems, Progr. Heat Mass Transfer 2 (1969) 1–12.

[6] P. Cannon, F.R. Steward, The calculation of radiative heat flux in a cylindrical furnace using the Monte Carlo method, Int. J. Heat Mass Transfer 14 (1971) 245–262.

[7] J.R. Howell, The Monte Carlo method in radiative heat transfer, J. Heat Transfer 120 (1998) 547–560.

[8] Z. Guo, S. Maruyama, Radiative heat transfer in inhomogeneous, nongray, and anisotropically scattering media, Int. J. Heat Mass Transfer 43 (2000) 2325–2336.

[9] J.G. Marakis, C. Papapavlov, E. Kakaras, A parametric study of radiative heat transfer in pulverised coal furnaces, Int. J. Heat Mass Transfer 43 (2000) 2961–2971.

[10] J.L. Consalvi, B. Porterie, J. Loraud, A formal averaging procedure for radiation heat transfer in particulate media, Int. J. Heat Mass Transfer 45 (2002) 2755–2768.

[11] S.C. Mishra, P. Talukdar, D. Trimis, F. Durst, Computational efficiency improvements of the radiative transfer problems with or without conduction—a comparison of the collapsed dimension method and the discrete transfer method, Int. J. Heat Mass Transfer 46 (2003) 3083–3095.

[12] J.G. Marakis, G. Brenner, F. Durst, Monte Carlo simulation of a nephelometric experiment, Int. J. Heat Mass Transfer 44 (2001) 989–998.

[13] L. Tessé, F. Dupoirieux, J. Taine, Monte Carlo modeling of radiative transfer in a turbulent sooty flame, Int. J. Heat Mass Transfer 47 (2004) 555–572.

[14] A.Y. Snegirev, Statistical modeling of thermal radiation transfer in buoyant turbulent diffusion flames, Int. J. Heat Mass Transfer 136 (2004) 51–71.

[15] D. Stankevich, Y. Shkuratov, Monte Carlo ray-tracing simulation of light scattering in particulate media with optically contrast structure, J. Quant. Spectrosc. Radiat. Transfer 87 (2004) 289–296.

[16] R. Vaillon, B.T. Wong, M.P. Mengüç, Polarized radiative transfer in a particle-laden semi-transparent medium via a vector Monte Carlo method, J. Quant. Spectrosc. Radiat. Transfer 84 (2004) 383–394.

[17] A. Battaglia, S. Mantovani, Forward Monte Carlo computations of fully polarized microwave radiation in non-isotropic media, J. Quant. Spectrosc. Radiat. Transfer 95 (2005) 285–308.

[18] S.W. Baek, D.Y. Byun, S.J. Kang, The combined Monte Carlo and finite volume method for radiation in a two-dimensional irregular geometry, Int. J. Heat Mass Transfer 43 (2000) 2337–2344.

[19] D. Byun, C. Lee, S.W. Baek, Radiative heat transfer in discretely heated irregular geometry with an absorbing, emitting and anisotropically scattering medium using combined Monte Carlo and finite volume method, Int. J. Heat Mass Transfer 47 (2004) 4195–4203.

[20] J.T. Farmer, J.R. Howell, Monte Carlo strategies for radiative transfer in participating media, Adv. Heat Transfer 31 (1998) 1–97.

[21] M. Kobiyama, Reduction of computing time and improvement of convergence stability of the Monte Carlo method applied to radiative heat transfer with variable properties, J. Heat Transfer 111 (1989) 135–140.

[22] J.T. Farmer, J.R. Howell, Hybrid Monte Carlo/diffusion methods for enhanced solution of radiative transfer in optically thick nongray media, Radiat. Heat Transfer: Curr. Res., ASME HTD 276 (1994) 203–212.

[23] J.T. Farmer, J.R. Howell, Monte Carlo algorithms for predicting radiative transfer in optically thick participating mediaTenth International Heat Transfer Conference, vol. 2, Taylor and Francis, Brighton, UK, 1994, pp. 37–42.

[24] D.V. Walters, R.O. Buckius, Rigorous development for radiation heat transfer in nonhmogeneous absorbing, emitting and scattering media, Int. J. Heat Mass Transfer 35 (1992) 3323–3333.

[25] D.V. Walters, R.O. Buckius, Monte Carlo methods for radiative heat transfer in scattering media, in: C.-L. Tien (Ed.), Annual Review of Heat Transfer, vol. 5, CRC Press, Boca Raton, 1994, pp. 131–176, chap. 3.

[26] B.X. Li, X.J. Yu, L. Liu, Backward Monte Carlo simulation for apparent directional emissivity of non-isothermal semitransparent slab, J. Quant. Spectrosc. Radiat. Transfer 91 (2005) 173–179.

[27] Y. Shuai, S.K. Dong, H.P. Tan, Simulation of the infrared radiation characteristics of high-temperature exhaust plume including particles using the backward Monte Carlo method, J. Quant. Spectrosc. Radiat. Transfer 95 (2005) 231–240.

[28] M. Cherkaoui, J.-L. Dufresne, R. Fournier, J.-Y. Grandpeix, A. Lahellec, Monte Carlo simulation of radiation in gases with a narrow-band model and a net-exchange formulation, J. Heat Transfer 118 (1996) 401–407.

[29] M. Cherkaoui, J.-L. Dufresne, R. Fournier, J.-Y. Grandpeix, A. Lahellec, Radiative net-exchange formulation within one-dimensional gas enclosures with reflective surfaces, J. Heat Transfer 120 (1998) 275–278.

[30] L. Tessé, F. Dupoirieux, B. Zamuner, J. Taine, Radiative transfer in real gases using reciprocal and forward Monte Carlo methods and a correlated-k approach, Int. J. Heat Mass Transfer 45 (2002) 2797–2814.

[31] A. de Lataillade, J.-L. Dufresne, M. El Hafi, V. Eymet, R. Fournier, A net-exchange Monte Carlo approach to radiation in optically thick systems, J. Quant. Spectrosc. Radiat. Transfer 74 (2002) 563–584.

[32] A. de Lataillade, S. Blanco, Y. Clergent, J.-L. Dufresne, M. El Hafi, R. Fournier, Monte Carlo method and sensitivity estimations, J. Quant. Spectrosc. Radiat. Transfer 75 (2002) 529–538.

[33] P. Perez, M. El Hafi, P.J. Coelho, R. Fournier, Accurate solutions for radiative heat transfer in two-dimensional axisymmetric enclosures with gas radiation and reflective surfaces, Numer. Heat Transfer, Part B 46 (2005) 39–63.

[34] V. Eymet, R. Fournier, S. Blanco, J.-L. Dufresne, A boundary-based net-exchange Monte Carlo method for absorbing and scattering thick media, J. Quant. Spectrosc. Radiat. Transfer 91 (2005) 27–46.

[35] J. Taine, J.-P. Petit, Transferts Thermiques. Introduction aux Sciences des Transferts, third ed., Dunod, Paris, 2003.

[36] R. Siegel, J.R. Howell, Thermal radiation heat transfer, third ed., Taylor and Francis, Washington, DC, 1992.

[37] H.C. Hottel, A.F. Sarofim, Radiative Transfer, McGraw-Hill, New York, 1967.

[38] R. Goody, R. West, L. Chen, D. Crisp, The correlated-k method for radiation calculations in nonhomogeneous atmospheres, J. Quant. Spectrosc. Radiat. Transfer 42 (1989) 539–550.

[39] A.A. Lacis, V. Oinas, A description of the correlated-k distribution method for modeling nongray gaseous absorption thermal emission and multiple scattering in vertically inhomogeneous atmospheres, J. Geophys. Res. 96 (1991) 9027–9063.

[40] P. Rivière, A. Soufiani, J. Taine, Correlated-k and fictitious gas methods for H_2O near 2.7 μm, J. Quant. Spectrosc. Radiat. Transfer 48 (1992) 187–203.

[41] P. Rivière, A. Soufiani, J. Taine, Correlated-k fictitious gas model for H_2O infrared radiation in the Voigt regime, J. Quant. Spectrosc. Radiat. Transfer 53 (1995) 335–346.

[42] A. Soufiani, J. Taine, High temperature gas radiative property parameters of statistical narrow-band model for H_2O, CO_2 and CO, and correlated-k model for H_2O and CO_2, Int. J. Heat Mass Transfer 40 (1997) 987–991.